Mineralogy and Characterization of New Bentonite from Tahoua Region of Central Niger

M. Gourouza[1,*], M. Harouna[2], A. Zanguina[1], I. Natatou[1] and A. Boos[3]

[1]Laboratoire Matériaux-Eaux-Environnement, Université Abdou Moumouni, BP: 10662 Niamey, Niger
[2]Laboratoire de géo ressources et hydrogéologie, Université Abdou Moumouni, BP: 10662 Niamey, Niger
[3]Analytical Laboratory, School of Chemistry of Polymers and Materials, Louis Pasteur University, Strasbourg, France

*Corresponding author: Tel: +227 96 408734; E-mail: gourouza.marou@yahoo.fr

Niger imports a huge quantity of bentonite, which it uses in mining and oil exploration, but also in village hydraulics. The objective of this study is the search for a bentonite-type clay deposit on the Nigerian territory. The clay fraction of a material collected on a clay deposit of the Paleocene Garadaoua Formation in the Ullemmeden basin (central Niger) was the subject of a series of analyzes: DRX; ICP-AES; ICP-MS; ATD-ATG; IR; Adsorption/desorption of N_2 at 77 K; cation exchange capacity, granulometry. DRX results corroborated by those of IR and ATD-ATG indicate that the clay minerals constituting the collected material are: montmorillonite, kaolinite and illite, with a strong predominance of montmorillonite. The mineralogical and chemical composition, the specific surface and the cation exchange capacity obtained indicate that the analyzed material is similar to that of Maghnia bentonite in Algeria.

Keywords: Clay, Mineralogy, Bentonite, Tahoua, Niger.

INTRODUCTION

Clays are used in many fields such as ceramics, paints, barriers, adsorbents, catalyst supports, drill bits, *etc*. [1-3]. The suitability of clay for its use in a specific field is related to its mineralogical and chemical composition [4-6]. Niger is full of considerable mining and petroleum potential, and exploration of this mining and petroleum potential requires the use of bentonite clay as a drill bit. This situation shows the need to investigate the clay deposits of Niger in search of bentonite. The aim is to characterize and identify a clay deposit of the Garadaoua Formation of Palaeocene in Ullemmeden basin (central Niger) [7]. Characterization and identification of the clay deposition is carried out on the basis of mineralogical, chemical and physico-chemical analyzes carried out on the collected material.

EXPERIMENTAL

The material is collected from Paleocene Garadaoua formation located in the Iullemmeden basin in Rey rey (Fig. 1). Paleocene Garadaoua formation consists of three lithostratigraphic series [7-11], namely (a) Lower argillaceous series

(lower papyraceous shales) called Kao limestone which is composed of silty claystones and palygorskite marls; (b) The limestone series called Tamaské member and composed of biomicritic limestones in sub-horizontal benches and finally (c) Upper argillaceous series (upper papyraceous shales), which is called as Barmou member, and comprising of alternative greenish argillites and nodulated phosphate s and dolomitic palygorskite marls.

Extraction of clay fraction: To separate the clay fraction (particles < 2 μm in diameter) from the investigated material, the material is grounded in agate and then disintegrated in demineralized water. The suspension is centrifuged at 2500 rpm for 10 min. The deflocculated suspension is transferred to a bottle. After 100 min of sedimentation, the upper layer of 2 cm of supernatant correspond to the fraction of < 2 μm is siphoned.

Characterization: The mineralogical composition of the collected material and its clay fraction is determined by X-ray diffraction using a RX Brüker diffractometer (model D5000), in 2θ mode (Scanning from 3° to 15° or 3 ° to 30 °, in steps of 0.02° with a duration of 1 s, anticathode Cu, 40 kV-30 mA). To dissociate the clay minerals from the clay fraction, four diffractograms are recorded from the following preparations:
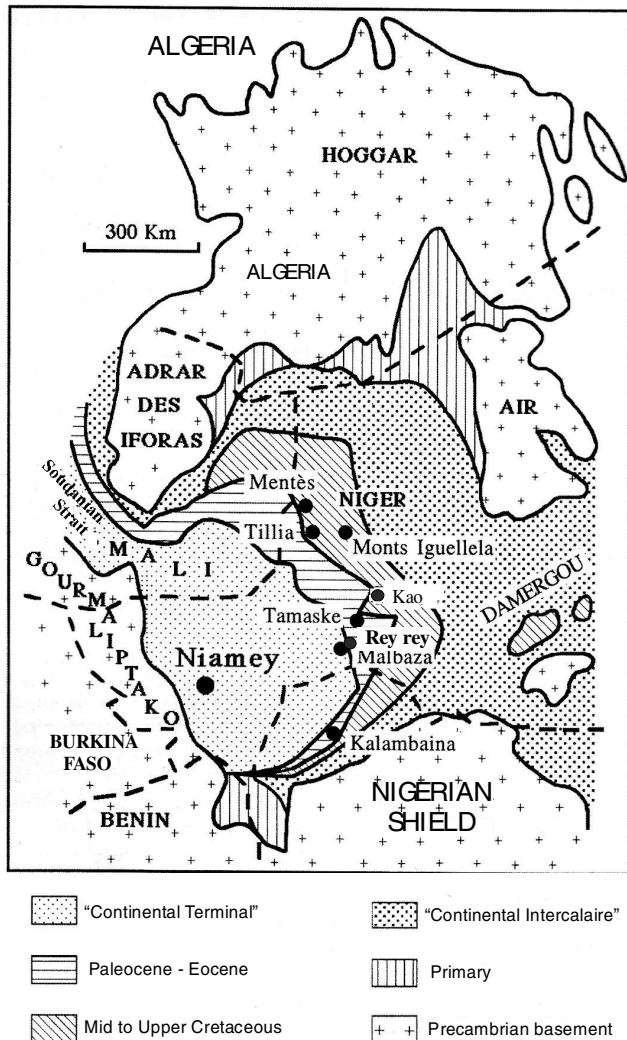
Fig. 1. Location of Rey rey sampling site on a simplified geological map of Iullemmeden basin (modified after Dikouma *et al.* [8])

(1) oriented preparation and dried in the open air; (2) oriented and treated with ethylene glycol, where the slides are placed overnight in a desiccators in an ethylene glycol atmosphere; (3) hydrazine-monohydrate oriented and treated preparation, where the slides are placed overnight in desiccators in hydrazine monohydrate atmosphere; and finally (d) heated for 4 h at 490 ℃.

Preparation: The siphoned clay fraction is centrifuged at 3500 rpm for 40 min. The pellet obtained is deposited on the edge of a grooved glass slide. The blades are dried in the open air [12-15]. The relative abundance of each clay mineral of the clay fraction is determined from the diffractogram of untreated preparation and using MacDiff software (version 4.1.2). An infrared spectrum of clay fraction is obtained using a Perkin Elmer Universal ATR (Attenuated Total Reflectance) spectrometer over a spectral range of 4000-600 cm^{-1}. Thermal decomposition of the clay fraction (ATG/ATD) is carried out using a thermal analyzer A 5c 1000c in air, in a temperature range of 25 to 1000 ℃. The specific surface area (total SA), area of micropores (micro SA) and pore volume (total PV) of the clay fraction are determined by adsorption/desorption of nitrogen at 77 K using a SORPTOMATIC 1990 of Thermoquest. The results were plotted by BET (Brunette-Emmett-Teller),

De Boer and BJH (Barrett-Joyner-Helenda) methods. Its cation exchange capacity (CEC) is determined by ion exchange in a solution of hexaaminecobalt(III) $[Co(NH_3)_6]^{3+}$ for three days [16,17]. The exchangeable cations (Na, K, Ca and Mg) expressed in meq per 100 g of clay fraction are measured using a Jobin Yvon Ultrace 138 model spectrometer (ICP-AES) [18]. Chemical analyzes of the clay fraction were carried out using two spectro-meters: an Agilent 7500 model (ICP-MS) and Jobin Yvon's Ultrace 138 (ICP-AES). The SiO$_2$ content is determined gravi-metrically.

RESULTS AND DISCUSSION

Granulometry: The granulometric distribution of particles of collected materials obtained by dispersion (Fig. 2) indicates that the particles with a diameter < 2 µm (clay fraction of sample) contained 23 % of the total particles.
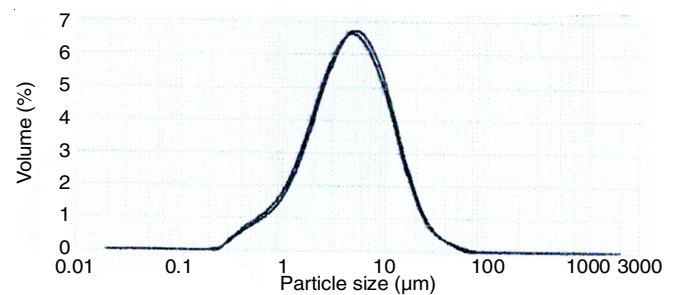

Fig. 2. Granulometric curve of collected material (MC)

X-ray diffraction analysis: The main reflections around 7, 10 and 15 Å diffractogram of untreated oriented prepared and dried in open air of the clay fraction of collected material (Fig. 3a) indicated the presence of kaolinite, illite and montmorillonite [5,19-21]. According to Rosenquist [22] and Bergaya [6], the reflection at 15 Å indicates that montmorillonite present in the sample is of calcium type. According to Hsieh [23] and Frederico *et al.* [24], the main refraction around 17 Å of prepared oriented treated with ethylene glycol (Fig. 3b) confirms the presence of montmorillonite. Indeed, in ethylene glycol vapour, water molecules of intermolecular space of montmorillonite are substituted by molecules of ethylene glycol. This substitution increases the interlayer distance and explains the appearance of main reflection around 17 Å in the diffractogram (Fig. 3c). Similarly, the main reflection around 10 Å is observed on all the diffractograms of oriented preparations (untreated, treated with ethylene glycol, treated with hydrazine or heated at 450 ℃) confirms the presence of illite in the sample analyzed. Indeed, illite is insensitive to indicated treatments. According to some researchers [12,25], the absence of principal reflection around 7 Å on the diffractogram of oriented heating at 450 ℃. Fig. 3d confirms the presence of kaolinite in the sample analyzed, since heated at 450 ℃ destroys the structure of kaolinite and explains the absence of its main reflection on the diffractogram (Fig. 3d). The percentages of kaolinite, illite and montmorillonite of the analyzed sample obtained following treatment of diffractogram of the untreated oriented preparation using MacDiff software (version 4.1.2) (Fig. 4) are: 60 % montmorillonite, 25 % kaolinite, 4 % illite and 11 % interstratified illite/montmorillonite. These percentages show a strong predo-
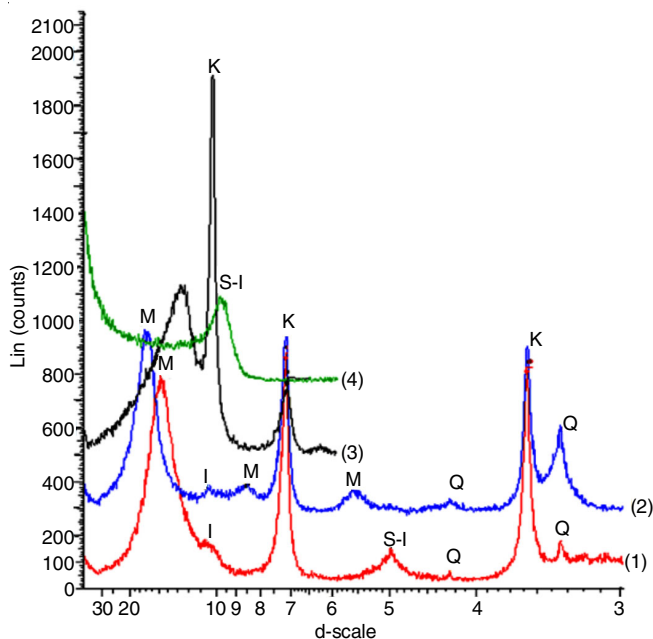
Fig. 3. XRD 1) oriented sample dried in the open air, 2) oriented sample treated with ethylene glycol, 3) oriented sample treated with hydrazine, and 4) a sample heated at 490°C for 4 hours (M = montmorillonite; K = kaolinite; I = illite; Q = quart; S-I = illite-smectite)
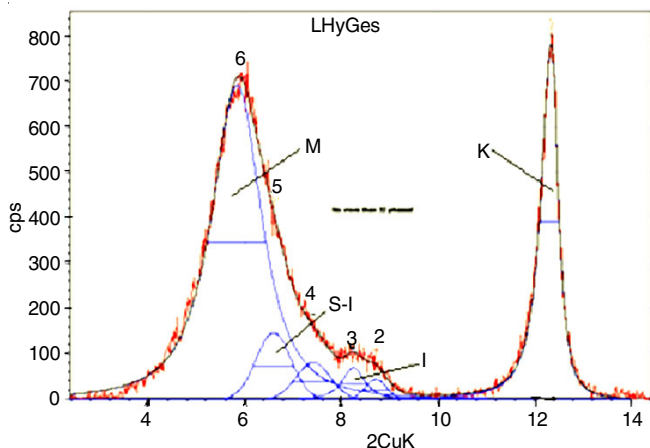

Fig. 4. Height reflections of relative abundance of clay minerals constituent (M = montmorillonite; K = kaolinite; I = illite; S-I = Smectite-illite)

minance in the analyzed sample of montmorillonite relatively to kaolinite and illite.

Infrared analysis: Some vibration modes provide important information on the structural characteristics of a material. Fig. 5 gives the infrared spectrum of the clay fraction of the collected material. The band at 692 cm^{-1} of infrared spectrum is attributable to the flexions and deformations of Si-O bonds of certain molecules of the sample analyzed [26-30]. According to Borchardt [26], the band at 1112 cm^{-1} is attributed to Si-O stretching vibrations of kaolinite. Similarly, the band at 3620 and 912 cm^{-1} shows the presence of montmorillonite in the sample analyzed and further indicated that it is in dioctahedral in shape [26]. The band at 1027 cm^{-1} is attributed to Si-O-Si moiety characteristics of bentonite tetrahedral sheets [24,29]. while the bands at 912 and 846 cm^{-1} are the characteristic bands of bending vibrations of Al-Al-OH and Al-Mg-OH groups of
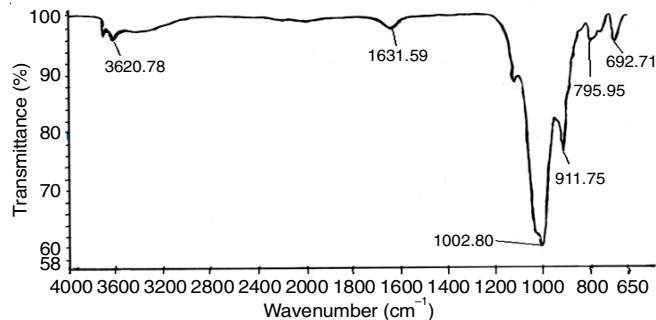

Fig. 5. Infrared spectrum of bedrock

bentonite [30-32]. The band at 3696 cm^{-1} is due to the vibrations in the inner surface hydroxide phase of the sample [33-38]. Finally, the bands at 830 and 750 cm-1 is attributed due to the presence of illite in the sample [39].

ATG/ATD curves: Fig. 6 shows the ATG/ATD curves of clay fraction of the sample. The peak around 100 °C of ATD curve ascribed to an endothermic reaction accompanied by a mass loss of about 7 % observed on the curve ATG [14,40]. While the peak at 100 °C of the ATD curve ascribed to an endo-thermic reaction indicating the loss of adsorbed water to the external surface and/or linked to the interchangeable cations of clay minerals of the sample [14,40]. This loss of adsorbed water explains the loss of mass of approximately 7 % of ATG curve and this peak at 100 °C proves the existence of the band at 3696 cm^{-1} in Fig. 5. The high intensity of peak around 100 °C indicate the presence of montmorillonite interstratified with illite [41].
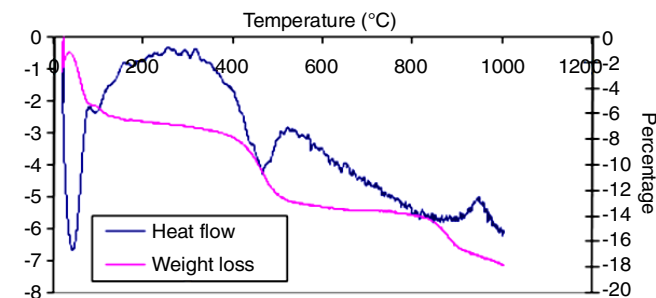

Fig. 6. TGA-TDA curve of bedrock

The endothermic peak at 400-600 °C of ATD curve of Fig. 6 indicates that montmorillonite of the sample might contain iron at an appreciable level [42]. The mass loss between 400-600 °C in the ATG curve is due to dehydroxylation of Al-Al-OH and Al-Mg-OH groups within the analyzed sample, according to reaction $2(OH) \longrightarrow H_2O + Or$ (r, residual) [14,43,44]. The exothermic peak at 950 °C in ATD curve indicates a crystal-lization of Al-Si spinel phase of kaolinite [45] similarly, dehyd-ration of illitic phase of analyzed sample also showed endo-thermic peaks at 56, 157 and 400 °C [46-48].

Adsorption/desorption with nitrogen: The hysteresis loop of analyzed sample (Fig. 7) can be assimilated to type H3 of IUPAC classification and type II [49], which indicates the presence of slotted pores, particles in sheets and majority of mesopores in the analyzed sample. The BET specific surface of the sample analyzed (91.36 m^2/g) proves its bentonitic character with intercalation cations Ca^{2+} and Mg^{2+} [50]. The surface of

<div style="text-align: center;">

TABLE-1

OXIDE CONTENT OF THE SAMPLE ANALYZED

</div>

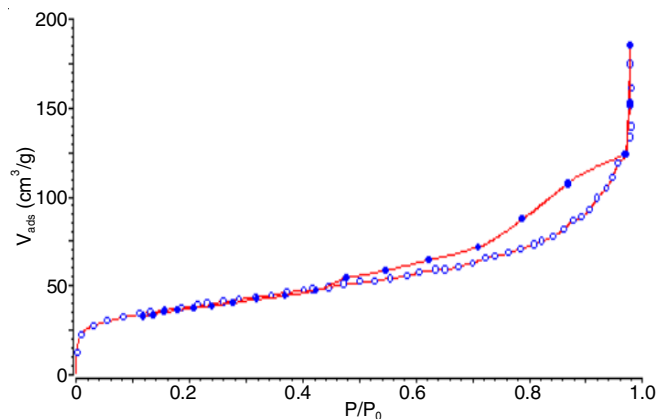| Oxide	SiO_2	Al_2O_3	Fe_2O_3	CaO	MgO	Na_2O	K_2O	TiO_2	Loss on fire	Total
Mass (%)	53.46	15.68	5.81	2.23	4.02	0.12	0.20	0.20	18	99.72

Fig. 7. Adsorption and desorption isotherms

DeBoer mesopores of the sample analyzed is found to be 45.48 m^2/g.

Chemical analysis: The oxide contents of the analyzed sample are shown in Table-1. The percentages of SiO_2 and Al_2O_3 in montmorillonite is almost same as according to the literature value [51]. The proportions of SiO_2 and Al_2O_3 in the sample analyzed are compatible to those of a natural bentonite used to adsorb uranium(IV) [52,53]. The cation exchange capacity of analyzed sample (0.66 meq/g) obtained by ion-exchange in a solution of $[Co(NH_3)_6]^{3+}$ is also found be similar to that of Maghnia bentonite in Algeria [32].

Conclusion

The identification and characterizations of a material from the clay deposit of Paleocene Garadaoua Formation in the Ullemmeden basin of central Niger are investigated. The XRD, IR and ATG/ATD results of the clay fraction indicate the presence of montmorillonite, kaolinite and illite with a strong predominance of montmorillonite. The strong predominance of montmorillonite, the CEC and the chemical composition of the material also indicate its calcium-like bentonite nature. Moreover, it good value of specific surface can be considered as good material for catalysis. The analyzed sample is also found to be compatible with some other bentonite *viz.*, Maghnia in Algeria.

CONFLICT OF INTEREST

The authors declare that there is no conflict of interests regarding the publication of this article.

REFERENCES

1. R.E. Grim and N. Güven, Bentonites-Geology, Mineralogy, Properties and Uses: Developments in Sedimentology, vol. 24, Elsevier: New York (1978).
2. H.H. Murray, *Appl. Clay Sci.*, **17**, 207 (2000); https://doi.org/10.1016/S0169-1317(00)00016-8.
3. F. Bergaya, B.K.G. Theng and G. Lagaly, Handbook of Clay Science. Development of Clay Science, vol. 1, Elsevier: Amsterdam (2006).
4. R.E. Grim, Clay Mineralogy, McGraw-Hill: New York, edn 2 (1968).
5. D.M. Moore and R.C. Reynolds, X-Ray Diffraction and the Identification and Analysis of Clay Minerals, Oxford University Press (1989).
6. F. Bergaya, B.K.G. Theng and G. Lagaly, eds., Handbook of Clay Science. Development of Clay Science, vol. 1, Chap.1, Elsevier: Amsterdam (2006).
7. M. Dikouma, Ph.D. Thesis, Fluctuations du niveau marin au Maastrichtien et au paléocène dans le bassin intracratonique des Iullemmeden, Ader-Doutchi, Niger Univ. Dijon-Niamey, p. 272 (1990).
8. M. Dikouma, J. Lang and A. Pascal, *Newsl. Stratigr.*, **29**, 105 (1993); https://doi.org/10.1127/nos/29/1993/105.
9. J. Greigert, Description des formations crétacées et tertiaires du bassin des Iullemmeden (Afrique occidentale), B.R.G.M. pp. 236 (1966).
10. M. Hanon, Cartes géologiques au 1/100.000 de l'Ader Doutchi (16 feuilles). DRGM Niger. AGCD Belgique (1984).
11. J. Soták, *Geol. Carpathica*, **61**, 393 (2010); https://doi.org/10.2478/v10096-010-0024-1.
12. G.W. Brindley and G. Brown, Crystal Structures of Clay Minerals and their X-ray Identification. Mineralogical Society, London (1980).
13. H. Chamayou and J.P. Legros, Les bases physiques, chimiques et mine'ralogiques de la science du sol. Presses Universitaires de France: Paris (1989).
14. K. Tan, Principles of Soil Chemistry, Marcel Dekker: New York, edn 2 (1991).
15. F. Wolters and K. Emmerich, *Thermochim. Acta*, **462**, 80 (2007); https://doi.org/10.1016/j.tca.2007.06.002.
16. I. Mantin, *C.R. Sci. Paris*, **1**, 815 (1969).
17. F. Bergaya and M. Vayer, *Appl. Clay Sci.*, **12**, 275 (1997); https://doi.org/10.1016/S0169-1317(97)00012-4.
18. P. Salerno and S. Mendioroz, *Appl. Clay Sci.*, **22**, 115 (2002); https://doi.org/10.1016/S0169-1317(02)00133-3.
19. M.L. Occelli, J.A. Bertrand, S.A. Gould and J.M. Dominguez, *Micropor. Mesopor. Mater.*, **34**, 195 (2000); https://doi.org/10.1016/S1387-1811(99)00173-0.
20. L.V. Amorim, C.M. Gomes, H.L. Lira, K.B. França and H.C. Ferreira, *Mater. Res.*, **7**, 583 (2004); https://doi.org/10.1590/S1516-14392004000400012.
21. A. Chakchouk, B. Samet and T. Mnif, *Appl. Clay Sci.*, **33**, 79 (2006); https://doi.org/10.1016/j.clay.2006.03.009.
22. I.Th. Rosenquist, *Nor. Geol. Tidsskr.*, **39**, 350 (1959).
23. Y.P. Hsieh, *Clays Clay Miner.*, **37**, 459 (1989); https://doi.org/10.1346/CCMN.1989.0370510.
24. F.G. Alabarse, R.V. Conceição, N.M. Balzaretti, F. Schenato and A.M. Xavier, *Appl. Clay Sci.*, **51**, 202 (2011); https://doi.org/10.1016/j.clay.2010.11.017.
25. E. Eslinger and D. Peaver, Clay Minerals for Petroleum Geologists and Engineers, SEPM Short course 22. Soc. Economic Paleontologists and Mineralogists, Tulsa, USA (1988).
26. L. Chen, Y. Huang, L. Huang, B. Liu, G. Wang and S. Yu, *J. Radioanal. Nucl. Chem.*, **290**, 675 (2011); https://doi.org/10.1007/s10967-011-1337-y.
27. J. Pan, C. Wang, S. Guo, J. Li and Z. Yang, *Catal. Commun.*, **9**, 176 (2008); https://doi.org/10.1016/j.catcom.2007.06.001.
28. J. Madejova, J. Bujdak, M. Janek and P. Komadel, *Spectrochim. Acta A Mol. Biomol. Spectrosc.*, **54**, 1397 (1998); https://doi.org/10.1016/S1386-1425(98)00040-7.

29. S. Caillére, S. Hénin and M. Rautureau, Minéralogie des Argiles. 1: structure et propriétés physico-chimiques. Masson: Paris (1982).

30. G.A. Borchardt, eds.: J.B. Dixon and S.B. Weed, Montmorillonite and Other Smectite Minerals. In: Minerals in Soil Environments. Soil Science Society of America, Madison: Wisconsin (1977).

31. S. Wang, Y. Dong, M. He, L. Chen and X. Yu, *Appl. Clay Sci.*, **43**, 164 (2009);
https://doi.org/10.1016/j.clay.2008.07.028.

32. S. Aytas, M. Yurtlu and R. Donat, *J. Hazard. Mater.*, **172**, 667 (2009);
https://doi.org/10.1016/j.jhazmat.2009.07.049.

33. S.T. Yang, D.L. Zhao, H. Zhang, S.S. Lu, L. Chen and X.J. Yu, *J. Hazard. Mater.*, **183**, 632 (2010);
https://doi.org/10.1016/j.jhazmat.2010.07.072.

34. P. Salerno, M.B. Asenjo and S. Mendioroz, *Thermochim. Acta*, **379**, 101 (2001);
https://doi.org/10.1016/S0040-6031(01)00608-6.

35. V.C. Farmer, The Infrared Spectra of Minerals, Mineralogical Society, Monograph 4, London (1974).

36. J.D. Russel and A.R. Fraser, ed.: M.J. Wilson, Infrared Methods in Clay Mineralogy: Spectroscopic and Chemical Determinative Methods Chapman and Hall: London (1996).

37. J. Madejova, *Vib. Spectrosc.*, **31**, 1 (2003);
https://doi.org/10.1016/S0924-2031(02)00065-6.

38. R.L. Ledoux and J.L.J. White, *J. Colloid Interface Sci.*, **21**, 127 (1966);
https://doi.org/10.1016/0095-8522(66)90029-8.

39. H.W. Van der Marel and H. Beutelspacher, Atlas of Infrared Spectroscopy of Clay Minerals and Their Admixtures; Elsevier: Amsterdam, The Netherlands (1976).

40. H. Van Olphen and J.J. Fripiat, Data Handbook for Clay Materials and Other Nonmetallic Minerals, Pergamon Press: Oxford (1979).

41. S. Guggenheim and A.F. Koster van Groos, *Clays Clay Miner.*, **49**, 433 (2001);
https://doi.org/10.1346/CCMN.2001.0490509.

42. E. Srasra, Thèse de 3ème cycle. Fac. Sc. Tunis. Univ. Tunis II (1987).

43. M.F. Brigatti, *Clay Miner.*, **18**, 177 (1983);
https://doi.org/10.1180/claymin.1983.018.2.06.

44. F. Ayari, E. Srasra and M. Trabelsi-Ayadi, *Desalination*, **185**, 391 (2005);
https://doi.org/10.1016/j.desal.2005.04.046.

45. M. Yurdakoç, M. Akçay, Y. Tonbul, F. Ok and K. Yurdakoç, *Micropor. Mesopor. Mater.*, **111**, 211 (2008);
https://doi.org/10.1016/j.micromeso.2007.07.032.

46. M. Alkan, B. Kalay, M. Dogan and Ö. Demirbas, *J. Hazard. Mater.*, **153**, 867 (2008);
https://doi.org/10.1016/j.jhazmat.2007.09.047.

47. Turkif, Ph.D. Thèsis, Université Louis Pasteur, Strasbourg, France (1987).

48. L.G. Berg, Introduction in Thermography, Publishing House of the Academy of Sciences of the USSR: Moscow (1961).

49. I. Kostov, Mineralogy, Tehnika Publishing House: Sofia (1993).

50. S. Brunauer, L.S. Deming, D.M. Deming and E. Teller, *J. Am. Chem. Soc.*, **62**, 1723 (1940);
https://doi.org/10.1021/ja01864a025.

51. S. Kaufhold, R. Dohrmann, M. Klinkenberg, S. Siegesmund and K. Ufer, *J. Colloid Interface Sci.*, **349**, 275 (2010);
https://doi.org/10.1016/j.jcis.2010.05.018.

52. M. Hayati-Ashtiani, *Part. Syst. Charact.*, **28**, 71 (2011);
https://doi.org/10.1002/ppsc.201100030.

53. O. Bouras, T. Chami, M. Houari, H. Khalaf, J.-C. Bollinger and M. Baudu, *Environ. Technol.*, **23**, 405 (2002);
https://doi.org/10.1080/09593332508618397.